

INVESTIGATION OF Pb-Li COMPATIBILITY FOR THE DUAL COOLANT TEST BLANKET MODULE— **B. A. Pint, J. L. Moser, and P. F. Tortorelli (Oak Ridge National Laboratory, USA)**

OBJECTIVE

The objective of this task is to assess the long-term, high-temperature compatibility of various materials with Pb-Li. One proposed fusion reactor concept uses SiC/SiC composites with a self-cooled Pb-17Li blanket. Another concept uses a SiC/SiC flow channel insert with a dual coolant of He and Pb-Li at ~800°C. This concept also requires tubing material to carry the Pb-Li between the first wall and the heat exchanger. As a first step in the evaluation process, monolithic SiC and potential tubing and coating materials are being exposed to Pb-17Li in capsule tests at 700°-1200°C.

SUMMARY

Static Pb-17Li capsule tests were performed on monolithic SiC specimens and Al-containing alloys. Both systems showed little or no dissolution in Pb-Li likely due to the formation of a protective surface oxide which was expected to be stable based on thermodynamic evaluations. For SiC, Si was detected in the Pb-Li only at the highest test temperatures (2,000h at 1100°C and 1000h at 1200°C). The addition of Al to Fe- or Ni-base alloys resulted in a significant decrease in the amount of dissolution after 1000h at 700° and 800°C compared to type 316 stainless steel. Chemical vapor deposited (CVD) aluminide coatings on type 316 substrates significantly reduced the dissolution rate at 800°C. With or without pre-oxidation, Al-containing alloys or coatings formed an Al_2O_3 surface layer. These results demonstrate that aluminide coatings could protect a conventional Fe- or Ni-base tubing alloy to carry Pb-Li between the first wall and the heat exchanger. Future work will need to include testing in a flowing system with a thermal gradient to fully determine the compatibility of these materials.

PROGRESS AND STATUS

Introduction

Among the proposed test blanket module (TBM) concepts for ITER, one possibility is a dual coolant (He and Pb-Li) system using advanced ferritic steels as the structural material and a silicon carbide composite as a flow channel insert.[1,2] Although the TBM design will operate at <500°C, thereby limiting compatibility problems, ultimately this concept would be more attractive with a maximum operating temperature of 700-800°C. In this temperature range, critical compatibility issues need to be addressed. Recent effort has been focused on the compatibility of ferritic-martensitic steels in Pb-Li at 400-600°C.[3,4] However, there has been less work examining SiC/SiC composites and corrosion-resistant coatings needed at higher temperatures.

The compatibility of SiC/SiC composites with Pb-17Li is of interest as a flow channel insert to reduce both corrosion and the MHD pressure drop and as a higher temperature (1000°-1100°C) structural material.[5] SiC dissolves readily in Li at <500°C.[6] However, the activity of Li is much lower in Pb-17Li (e.g., 1.2×10^{-4} at 500°C)[7] such that the native surface oxide on SiC, SiO_2 , is stable. The same argument applies for Al-containing alloys or coatings that could form a protective external Al_2O_3 in Pb-Li.[8] Coatings are of interest for tubing materials to carry Pb-Li from the first wall to the heat exchanger at ~700°C. While a SiC flow channel insert could protect the steel walls from Pb-Li dissolution, it is unlikely this strategy could be used through the entire flow path. Contact of Fe- or Ni-base, alloys with flowing Pb-Li at this temperature would result in unacceptably high dissolution rates.[3,4,9] Although the use of refractory metals is one option,[10] fabrication and durability of Nb or Mo tubing could be an issue. A protective coating could allow a conventional Fe- or Ni-base tubing alloy to be used.

Baseline compatibility data is being developed using static capsule tests and model materials. Studying monolithic SiC avoids issues with composites, such as fiber interfaces and porosity. Initially, a range of Al-containing alloys were studied. Based on positive results at 700°C, CVD aluminide coatings on type 316 stainless steel substrates were tested at 800°C. Both sets of experiments show promising results, consistent with the thermodynamic assessment.

Experimental Procedure

Capsule tests with static PbLi (detailed elsewhere[11]) were performed on dense, monolithic, high-purity (99.9995%) chemical vapor deposited (CVD) γ -SiC specimens (3 x 8 x 12 mm) with a density of 3.21g/cm³. To avoid unwanted reactions, the SiC specimen and Pb-Li were contained in CVD SiC capsules and welded Mo intermediate capsules. The 1200°C experiment used an outer capsule of alloy 602CA (Ni-26at%Cr-9Fe-5Al). In all tests, the capsules were loaded with high purity (99.9999%) Pb shot and Li in an argon-filled glove box. Specimen mass was measured before and after exposure on a Mettler-Toledo balance with an accuracy of ± 0.04 mg. Exposures were performed in resistively heated box furnaces.

The chemical composition of the Al-containing alloys tested at 700° and 800°C are shown in Table I. A Fe₃Al composition was selected as being similar to aluminide coatings formed on Fe-base alloys[12-14] and a Ni-42Al composition is similar to the composition of a CVD aluminide coating on a Ni-base alloy.[15] In addition, an oxide dispersion strengthened (ODS) FeCrAl (Plansee alloy PM2000) was tested as this alloy, or similar commercial tubing alloys (e.g. Kanthal alloy APMT),[16] could be used without a coating. The 1.5mm thick specimens had a surface area of 4-5cm² and were polished to a 600grit SiC finish. The alloy specimens were not pre-oxidized before testing at 700°C but were pre-oxidized for 2h at 1000°C in 1 atm dry O₂ before exposure at 800°C. Two specimens of type 316 stainless steel were CVD aluminized for 4h at 1050°C in a laboratory scale reactor and then immediately annealed for 2h at the same temperature.[13,14] These conditions produce a coating approximately 200 μ m thick with an Al-rich outer layer, \sim (Fe,Ni)₃Al, about 20 μ m thick. All metal specimens were ultrasonically cleaned in acetone and methanol prior to suspending the specimens in a welded Mo (or steel) capsule using Mo (or steel) wire.

After exposure, the specimens were soaked in a mixture of acetic acid, hydrogen peroxide and ethanol for 24-72h to remove any residual Pb-Li. The composition of the Pb-Li after testing was determined by inductively coupled plasma analysis and combustion analysis. Post-test surfaces were examined using Auger electron spectroscopy (AES), x-ray photoelectron spectroscopy (XPS) and secondary electron microscopy (SEM). Cross-sections of the metal specimens were examined using electron probe microanalysis (EPMA).

Table 1. Alloy chemical compositions (atomic% or ppma) determined by inductively coupled plasma analysis and combustion analysis

Material	Fe	Ni	Cr	Al	O	C	N	S	Other
316SS	65.1	8.9	19.9	0.02	490	3360	2380	68	1.94Si, 1.67Mn, 1.38Mo, 0.21Cu
ODS FeCrAl	67.8	0.02	20.0	10.6	7430	340	210	50	0.44Ti, 0.23Y, 0.04Si, 0.04Mn
Fe-28Al-2Cr+Zr	70.0	<	2.0	27.9	70	400	<	46	0.026Zr, 0.005Hf
Ni-42.5Al	<	57.3	<	42.6	40	380	<	<	<

< indicates below the detectability limit of <0.01% or <0.001% for interstitials

Results and Discussion

SiC Specimens. Three capsule experiments with monolithic SiC specimens exposed have recently been completed: 5,000h at 800°C, 2,000h at 1100°C and 1,000h at 1200°C. A summary of the mass change results for the most recent capsule tests and previous tests[11,17] is shown in Table 2. A statistically significant mass gain was observed after 5,000h at 800°C while the other tests showed smaller mass gains or losses. Limited reaction at 800°C is consistent with previous results.[18,19] No change in the specimen surface was visible. However, as with the earlier tests, a small amount of powdery black residue was left on the specimen surface. This was identified as C by AES with trace amounts of Pb and Li detected by XPS.

The composition of the Pb-Li after exposure is shown in Table 3. Although previous tests had shown no detectable Si after exposures for 1,000h at 800°C and 1100°C, Si was detected after 2,000h at 1100°C and 1,000h at 1200°C. (The amount does not necessarily correspond to the specimen mass change because the capsule was made of the same CVD SiC.) The presence of Si in the Pb-Li indicates that some dissolution occurred at the higher temperatures and suggests that SiC may be limited to <1100°C in flowing Pb-Li. These Si levels are still less than the 2100ppma (350ppmw) that was reported from EPMA of Pb-Li after an 800°C exposure.[19] The O, C and N contents increased after each exposure, however, some contamination could occur during post-test handling. Capsule experiments are being planned with SiC/SiC composite specimens. More interaction may be expected with the SiC fibers or the fiber-matrix interface, however, it is anticipated that a dense CVD SiC seal coat will cover the outer layer of any SiC composite components.[5]

Metallic Specimens. Table 4 shows the mass losses for the Al-containing alloys exposed for 1,000h at 700°C in Pb-17Li compared to the mass loss for type 316 stainless steel in three different types of

Table 2. Mass change of CVD SiC specimens after exposure in Pb-17Li

Temperature	Time	Mass Change	
		(mg)	(mg/cm ²)
800°C	1,000h	-0.02 ±0.04	-0.01 ±0.01
	5,000h	+0.10	+0.03
1100°C	1,000h	-0.02	-0.01
	2,000h	+0.02	+0.01
1200°C	1,000h	+0.04	+0.01

Table 3. Chemical composition using inductively coupled plasma and combustion analysis of the starting Pb and the Pb-Li after capsule exposures at the indicated temperatures and times (in ppma except for Li in atomic%)

Test	Li	Si	C	O	N	Al	Cr	Fe	Mo	Ni	Y
Starting	n.d.	<40	<170	1270	<40	<8	<4	<4	<2	<4	<2
1,000h exposure											
800°C	17.49%	<30	1850	4090	100	6	<3	6	<2	<3	<2
1100°C	16.27%	<30	1160	3550	90	<6	<3	6	<2	<3	<2
1200°C	15.62%	370	2690	16620	450	<20	<10	<10	<5	<10	<6
2,000h exposure											
1100°C	15.99%	185	1025	7890	200	<60	<30	<30	<20	<30	<20
5,000h exposure											
800°C	18.55%	<60	650	2580	90	<20	<10	<10	<5	<10	<6

Table 4. Mass change of specimens after 1000h at 700°C in Pb-17Li

Specimen	Capsule	Mass Change	
		(mg)	(mg/cm ²)
316SS	316SS	-3.1	-0.67
316SS	Fe	-26.2	-5.72
316SS	Mo	-17.4	-3.79
ODS FeCrAl	Mo	-1.4	-0.20
Fe-28Al-2Cr+Zr	Mo	-1.0	-0.25
Ni-42.5Al	Mo	-0.4	-0.09

capsules.[20] Compared to type 316 stainless steel, more than an order of magnitude reduction in the amount of dissolution was observed. The lowest mass loss for a 316SS specimen was in the 316SS capsule. This can be understood based on the fundamental flux equation governing dissolution in a liquid metal like Pb-Li:

$$J_i = k (C_i^S - C_i) \quad [1]$$

where J_i is the flux of species i into (positive) or from (negative) the liquid metal, C_i^S is the solubility of i in the Pb-Li and C_i is the instantaneous concentration of i in the liquid. In a capsule experiment, dissolution continues until the liquid metal is saturated, i.e. $C_i^S = C_i$. Therefore, with a 316SS capsule, the predominant dissolution of Ni and Cr would reach saturation quickly due to the large surface area of the capsule itself (relative to the specimen). This correlates well with the high levels of Ni, Mn and Cr observed in the Pb-Li from this capsule, Table 5. In contrast, with a Fe or Mo capsule all of the Ni and Cr needed to reach saturation would come from the 316SS specimen. Thus the higher mass losses for these tests are expected.

All of the specimens were characterized after exposure and Figures 1-4 give examples of those findings. Figure 1 shows a polished cross-section of the type 316 stainless steel specimen after exposure. As expected, there is an outer layer depleted in both Cr (Figure 1b) and Ni (Figure 2). The mass loss corresponds to a ~5µm loss in metal, with Ni and Cr being selectively removed, which is consistent with this observation. The Mo-rich precipitates in the outer layer (Figure 1c) are not likely from the Mo capsule, but from the alloy itself, Table 1. Figure 3 shows a similar Mo map from the 316SS specimen exposed in a carbon steel capsule at 700°C. Similar Mo-rich particles are present in the outer layer without an external source of Mo.

No depletion layer was observed in the NiAl specimen although selective removal of Ni would be expected. However, a slight depletion in Al was observed near the surface that may be due to Al diffusing outward

Table 5. Chemical composition using inductively coupled plasma and combustion analysis of the starting Pb and the Pb-Li after capsule exposures at 700°C for 1000h (in ppma except for Li in atomic%)

Test	Li	Fe	Cr	Ni	Mn	Si	Al	Mo	C	O	N	S
Starting	n.d.	<4	<4	<4	<4	<40	<8	<2	<170	1270	<40	<50
316SS (SS)	16.4%	60	160	740	380	<60	<60	<20	1420	4810	160	320
316SS (FS)	17.3%	30	<30	90	30	<60	<60	<20	970	3346	40	110
316SS (Mo)	17.4%	<30	<30	90	<30	<60	<60	<20	1590	7440	60	903
FeCrAl (Mo)	17.9%	30	<30	<60	<30	<60	<60	<20	1260	4140	90	370
Fe ₃ Al (Mo)	16.5%	<30	<30	<60	<30	<60	<60	<20	1520	14860	320	110
NiAl (Mo)	18.2%	840	<30	30	<30	<60	<60	20	1200	10310	370	1100

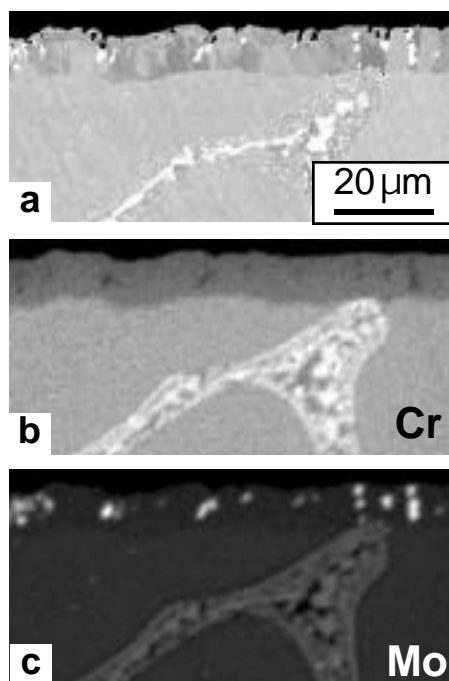


Fig. 1. (a) Secondary electron image of a polished cross-section of type 316 stainless steel after exposure in a Mo capsule for 1,000h at 700°C in Pb-17Li. X-ray maps of the same region show the concentration of (b) Cr and (c) Mo. The Cr- and Mo-rich second phase in the steel is likely sigma or a laves phase.

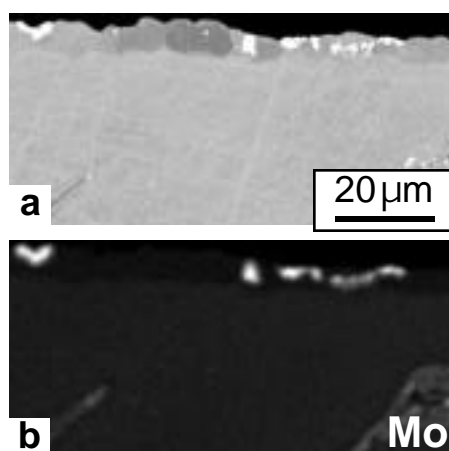


Fig. 3. (a) Secondary electron image of a polished cross-section of type 316 stainless steel after exposure in a carbon steel capsule for 1,000h at 700°C in Pb-17Li. X-ray maps of the same region show the concentration of (b) Mo.

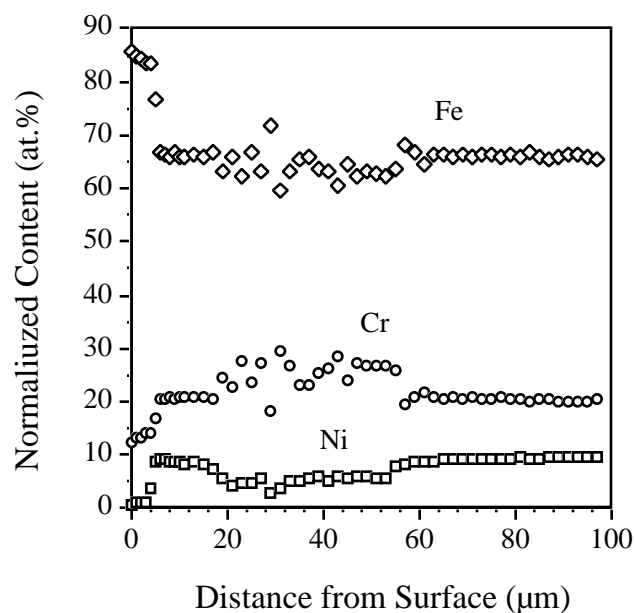


Fig. 2. Composition line profile of a polished cross-section of type 316 stainless steel after exposure for 1,000h at 700°C in Pb-17Li. The Ni and Cr are depleted from the outer region shown in Figure 1a.

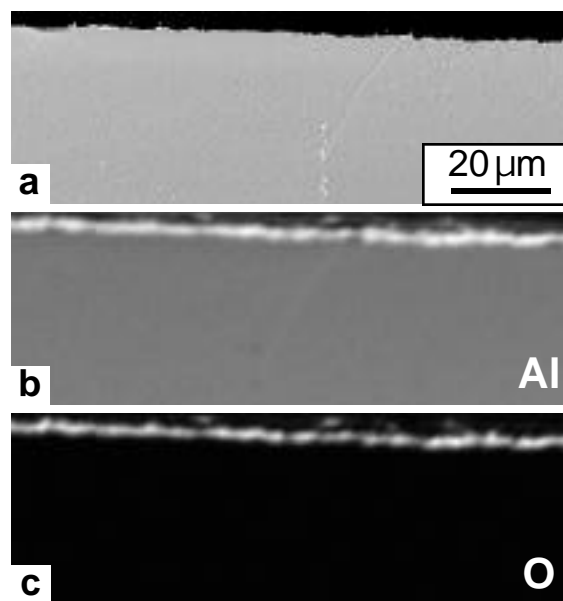


Fig. 4. (a) Secondary electron image of a polished cross-section of Ni-42Al after exposure for 1,000h at 700°C in Pb-17Li. X-ray maps of the same region show the concentration of (b) Al and (c) O.

Table 6. Mass change of specimens after 1000h at 800°C in Pb-17Li with a Mo capsule

Specimen	Pre-oxidation	Mass Change	
		(mg)	(mg/cm ²)
316SS	none	-79.51	-17.30
316SS + CVD Al	none	- 1.55	- 0.34
316SS + CVD Al	2h at 800°C	- 1.93	- 0.43
ODS FeCrAl	2h at 1000°C	+ 1.58	+ 0.24
Fe-28Al-2Cr+Zr	2h at 1000°C	- 1.55	- 0.37
Ni-42.5Al	2h at 1000°C	-12.12	- 2.72

to form a surface Al_2O_3 layer, Figures 4b and 4c. Similar oxide layers, although less distinct, were observed on the FeCrAl and Fe_3Al specimens. This is a relatively low temperature for the formation of a continuous alumina layer. With the lower Al contents in FeCrAl and Fe_3Al , these specimens may not have been able to form an alumina layer as quickly. The higher mass losses for these materials (Table 4) may be associated with the longer time needed to form a protective alumina layer by gettering O from the Pb-Li.

Table 6 shows the initial mass change results for a series of capsules run for 1,000h at 800°C. In this case, all of the capsules were Mo and the Al-containing alloys and one of the aluminized 316SS specimens were pre-oxidized, Table 6. Compared to the uncoated 316SS specimen, the aluminized 316SS specimens showed dramatically lower mass losses. Pre-oxidizing the coating for 2h at 800°C to form an alumina layer did not have a beneficial effect on dissolution. The Al-containing alloys also showed lower amounts of dissolution. The mass gain for the ODS FeCrAl specimen may be due to entrapped metal, however, the specimen appeared unaffected by the exposure. The Fe_3Al specimen had one ~3mm area where the oxide was removed causing some degree of mass loss. This selective attack area may be due to incomplete initial mixing of the Pb and Li. Lithium would quickly attack alumina and any of these alloys at 800°C. The highest mass loss was for NiAl where ~90% of the oxide appeared to be spalled after exposure. One reason for the higher mass loss may be that Ni dissolves more readily than Fe in PbLi. Another factor is that this alloy did not contain a reactive element addition (e.g. Y, Zr, Hf, etc.) which improves the adhesion of the alumina layer formed during pre-oxidation, Table I. Spallation of the alumina could have allowed more attack for this specimen. This experiment could be repeated with Hf-doped NiAl specimen to test this hypothesis.

Future work will eventually include flowing liquid metal experiments with a temperature gradient. Static capsule experiments can only be expected to produce a limited assessment of the compatibility issue because saturation inhibits further dissolution, Equation 1. Since low-cost quartz loops have been used for testing Bi-Li,[21] the possibility of constructing Pb-Li loops out of quartz was investigated by testing Pb-17Li in a quartz ampule at 800°C. The post-test PbLi chemistry is being measured to determine if any dissolution of the quartz occurred during this exposure.

References

- [1] P. Noajitra, L. Buhler, U. Fischer, S. Malang, G. Reimann, and H. Schnauder, Fusion Eng. Des. 61-62 (2002) 449.
- [2] M. Abdou, D. Sze, C. Wong, M. Sawan, A. Ying, N. B. Morley, and S. Malang, Fusion Sci. Technol. 47 (2005) 475.
- [3] G. Benamati, C. Fazio, and I. Ricipito, J. Nucl. Mater. 307-311 (2002) 1391.
- [4] J. Konys, W. Krauss, Z. Voss, and O. Wedemeyer, J. Nucl. Mater. 329-333 (2004) 1379.
- [5] B. Riccardi, L. Giancarli, A. Hasegawa, Y. Katoh, A. Kohyama, R. H. Jones, and L. L. Snead, J. Nucl. Mater. 329-333 (2004) 56.

- [6] T. Yoneoka, S. Tanaka, and T. Terai, *Mater. Trans.* 42 (2001) 1019-1023.
- [7] P. Hubberstey, *J. Nucl. Mater.* 247 (1997) 208.
- [8] P. Hubberstey, T. Sample, and A. Terlain, *Fusion Technol.* 28 (1995) 1194.
- [9] T. Flament, P. Tortorelli, V. Coen, and H. U. Borgstedt, *J. Nucl. Mater.* 191-194 (1992) 132.
- [10] H. Feuerstein, H. Gräbner, J. Oschinski, and S. Horn, *J. Nucl. Mater.* 233-237 (1996) 1383.
- [11] B. A. Pint, L. D. Chitwood, and J. R. DiStefano, DOE/ER-0313/35 (2003) 13.
- [12] N. V. Bangaru and R. C. Krutenat, *J. Vac. Sci. Technol. B2* (1984) 806.
- [13] Y. Zhang, B. A. Pint, J. A. Haynes, I. G. Wright, and P. F. Tortorelli, *Oxid. Met.* 62 (2004) 103.
- [14] Y. Zhang, B. A. Pint, G. W. Garner, K. M. Cooley, and J. A. Haynes, *Surf. Coat. Technol.* 188-189 (2004) 35.
- [15] Y. Zhang, W. Y. Lee, J. A. Haynes, I. G. Wright, B. A. Pint, K. M. Cooley, and P. K. Liaw, *Met. Trans.* 30A (1999) 2679.
- [16] B. Jönsson, R. Berglund, J. Magnusson, P. Henning, and M. Hättestrand, *Mater. Sci. Forum*, 461-464 (2004) 455.
- [17] B. A. Pint, J. L. Moser, and P. F. Tortorelli, *Fusion Engineering and Design* (in press).
- [18] F. Barbier, Ph. Deloffre, and A. Terlain, *J. Nucl. Mater.* 307-311 (2002) 1351.
- [19] H. Kleykamp, *J. Nucl. Mater.* 321 (2003) 170.
- [20] B. A. Pint, P. F. Tortorelli, and J. L. Moser, DOE-ER-0313/38 (2005) 89.
- [21] J. R. DiStefano and O. B. Cavin, Report # ORNL/TM-5503, Oak Ridge National Laboratory, Oak Ridge, TN (1976).